A μ-MAGNETOMETER BASED ON ELECTRON TUNNELING

L.M. Miller, J.A. Podosek, E. Kruglick,
Center for Space Microelectronics Technology, Jet Propulsion Laboratory,
California Institute of Technology, Pasadena, CA

T.W. Kenny
Department of Mechanical Engineering,
Stanford University, Stanford, CA

J.A. Kovacich
Eaton Corporation
Milwaukee, WI

W.J. Kaiser
Electrical Engineering Department
University of California, Los Angeles
Los Angeles, CA

ABSTRACT

In this paper, a working prototype of a μ-magnetometer based on electron tunneling is described. The tunneling μ-magnetometer offers a unique combination of advantages including high resolution (~10^{-9} Tesla/√Hz), vector sensitivity, wide bandwidth (> 10 kHz), low power (<100 mW), small size (1 cm X 1 cm X 0.6mm), robustness, wide dynamic range (>100 dB), and small temperature coefficient. The preliminary mist equivalent magnetic field (NEB) for a prototype is 6 μT/√Hz, in good agreement with a device performance model. Linear response to increasing DC and ac magnetic fields is also demonstrated. 1 finally, work in progress to improve the NEB to 4 nT/√Hz is described.

INTRODUCTION

The goal of this work is to develop a .? axis magnetometer which can be integrated into a semi-autonomous 10 cm-sized free flying magnetometer spacecraft to measure magnetic fields on the order of a nT [1]. This 10 cm spacecraft would be ejected from an orbiting platform, carry out B field measurements, and transmit the data back to the orbiting platform for relay to ground. In addition to nT resolution this application imposes severe requirements on the overall size (cm^3), power (consumption (<100 mW), vector sensitivity, radiation and thermal immunity, and bandwidth (100 Hz) of the magnetometer. For commercial applications, the magnetometer must also be inexpensive, reliable, and possesses a wide dynamic range. Although the superconducting quantum interference device (S QUID) [2,3] provides the most sensitive magnetic measurement, SQUID's also require significant power for cooling. Other magnetometers have also been studied for this application. Flux gate magnetometers, magnetoresistors, and magnetotransistors are currently being examined as candidate magnetometers, but do not yet meet the full set of mission requirements [4].

The tunneling μ-magnetometer, described in this work, offers a unique combination of advantages including high resolution (~10^{-9} Tesla), vector sensitivity, wide bandwidth (> 10 kHz), low power (< 100 mW), small size (1 cm X 1 cm X 0.6mm), robustness, wide dynamic range (>100 dB), and small temperature coefficient. In this paper, the development of the μ-magnetometer based on an electron tunneling transducer [5-7] is described. The electron tunneling transducer, μ-magnetometer prototype design and characterization, and follow-on research goals are discussed in detail.

ELECTRON TUNNELING TRANSDUCER

The electron tunneling transducer [5 7] is based on scanning tunneling microscopy (STM) which is used to study atomic surface structures [8] In this technique an atomically sharp, conductive tip is biased at a small potential and brought into close proximity (~10 Å) of a conductive, typically grounded, surface. At this small gap spacing, electrons are allowed to quantum mechanically tunnel across the vacuum barrier separating the tip and the conductive surface. This electron tunneling current is exponentially dependent on the gap spacing, Z, between the tip and the surface,

$$I_{tunneling} = I_0 \exp(-\alpha Z \sqrt{\Phi}) \qquad (1)$$

where $\alpha = 1.025\ eV^{-1/2}Å^{-1}$, and Φ is the potential barrier between the tip and the conductive surface. Typical tunneling currents are in the nA range with a gap sensitivity in the sub-mÅ range.

Scanning tunneling microscopy has been extended to displacement transducers in the development of the silicon micromachined tunneling transducer [5 7]. A cross-section of the tunneling transducer with control electronics is shown schematically in Figure 1.

The device is bulk-micromachined entirely from silicon, and consists of a silicon substrate which supports a fixed electron tunneling tip and a deflection electrode, and a flexible, low-stress silicon nitride membrane ($2.5 \times 2.5\ mm^2$) which supports a counter deflection electrode. All contacts are gold and the device operates in ambient (air) conditions. A voltage is applied to the electrostatic actuator electrode which pulls the flexible membrane to within ~10Å of the tunneling tip and allows electrons to quantum mechanically tunnel across the air gap barrier. A preamplifier stage converts the electron tunneling current to a tunneling voltage. The tunneling voltage is then compared to a preset value. The output of the comparator is then fed back onto the electrostatic actuator to produce a wide bandwidth force-rebalance network. The output of the comparator, Vt, is linearly proportional to forces, F_Z, perpendicular to the membrane, Wide bandwidth operation (>10 kHz) and wide dynamic range (>100 dB) are typical in this configuration [5].

The dominant noise in the tunneling transducer is a 1/f power spectrum (~$1/\sqrt{f}$ in the voltage. noise spectrum). A typical Hoist spectrum is shown in Figure ?. The presence of 1/f noise *normally* precludes DC operation of tunneling sensors. A solution to this problem is addressed in a later section.

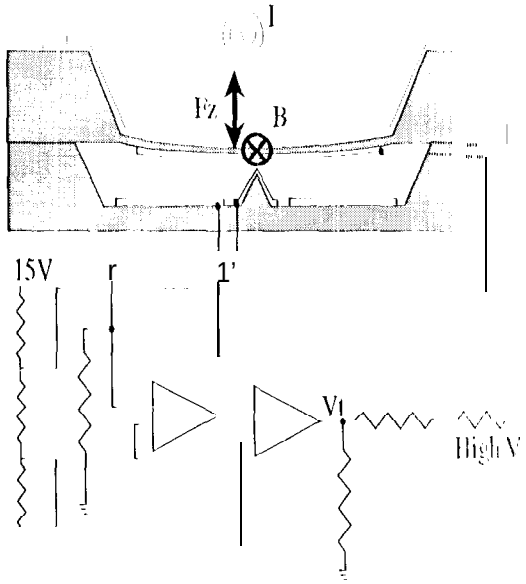

Figure 1. Schematic of electron tunneling magnetometer. A magnetic field, B, perpendicular to the current, Iac, produces a Lorentz force, F', which is monitored by the electron tunneling transducer.

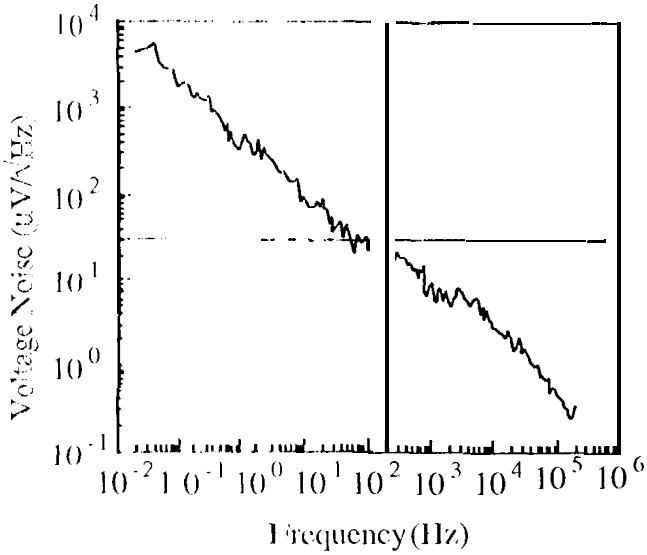

Figure 2. Typical noise spectrum of a silicon micromachined tunneling transducer, showing the operating point for a measurement chopped at 200117,.

μ-MAGNETOMETER DESIGN

The tunneling transducer is converted to a magnetometer by fabricating a wire coil on top of the flexible membrane as shown schematically in Figure 1. The wire coil is positioned such that the wire segments supported by the membrane are straight line segments as demonstrated in Figure 3 of the top view schematic of the tunneling μ-magnetometer. When a current passes through the wire coil, a Lorentz force is produced,

$$F = nlIBsin\theta, \qquad (2)$$

where n is the number of loops in the coil, l is the length of the wire segment supported by the membrane, I is the current through the wire coil, B is the magnetic field, and θ is the angle between the magnetic field vector and the wire segments supported by the membrane. In this device, an oscillating current is applied to the wire coil. Therefore, the Lorentz force generated by interaction with the magnetic field oscillates at the bias frequency. This is very important because it allows the tunneling transducer to measure a static quantity (B field), by detecting the *amplitude* of a force oscillation. Low-frequency noise in the transducer is therefore inconsequential to the measurement; only the noise at the bias frequency is relevant. For example, an ac current passing through the wire coil at a frequency of 200 Hz will effectively shift the operating point of the tunneling μ-magnetometer to a low noise portion of the noise spectrum as shown in Figure 2.

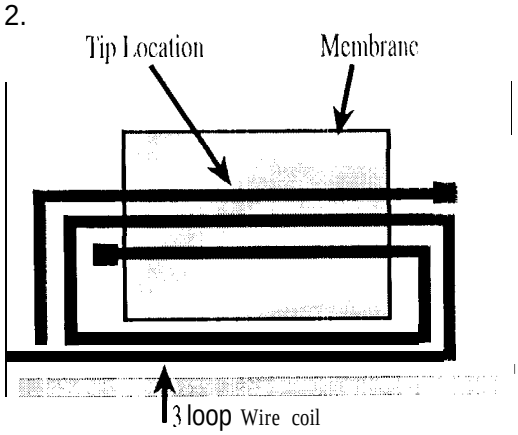

Figure 3. Top view schematic of tunneling μ-magnetometer showing 3 loop wire coil fabricated across a low-stress silicon nitride thin film.

For the design of the first prototype, we selected a simple design incorporating a single current loop, a 2.5 mm x 2.5 mm membrane, and 30 μm tip. The minimum detectable magnetic field, NEB, for the prototype design, can be calculated,

$$NEB = \frac{\text{voltage noise}}{(\text{transducer responsivity})(\text{Lorentz response})}$$

$$= \frac{35\ \mu V/\sqrt{Hz}}{(5 \times 10^{-5}\ V/N)(2.5 \times 10^{5}\ /T)}$$

$$2.8\ \mu T/\sqrt{Hz}. \qquad (3)$$

where voltage noise and transducer responsivity are measured parameters for the prototype, and the Lorentz response to magnetic field is nIL (See Equation 2).

RESULTS/DISCUSSION

The prototype μ-magnetometer was mounted in a non-magnetic package on a PC board containing the force-rebalance network shown in Figure 1. The PC board was then placed in a Helmholtz coil and oriented such that the magnetic field vector was perpendicular to the wire coil line segments and in the plane of the membrane. The Helmholtz coil was shielded from the environment with two levels of μ-metal shielding. Calibrated current sources were used both for the bias current on the tunneling μ-magnetometer and the Helmholtz coil. The output of the μ-magnetometer, Vt, was monitored using a dynamic signal analyzer which was triggered off the bias current for the μ-magnetometer. A calibrated flux gate magnetometer was used as a reference sensor.

A typical output response of the tunneling μ-magnetometer is shown in Figure 3 for a small DC magnetic field, B_{DC}, and an ac magnetic field at 10 Hz, B_{ac}. Because the bias current in the wire coil is biased at 196117, the response to B_{DC} is a peak in the Fourier spectrum at 196 Hz, and the response to B_{ac} is two peaks at 196 ± 10117. The NEB for the prototype was measured at 6.6 μT/√Hz. This is in good agreement with the theoretical calculation of 2.8 μT/√Hz, which is limited by an estimated value of the mass of the membrane used in the calculation of the transducer force sensitivity.

The prototype μ-magnetometer response to I, B_{DC}, and B_{ac} are shown in Figures 4, 5, and 6 respectively. As predicted by the Lorentz force expression, Equation 2, excellent linear response to the bias current and the magnetic field fire.(iclllolls(t;it~'(i experimentally. In the case of the response to I, the tunneling μ-magnetometer was biased at 400 Hz in a ac magnetic field (900 μT, 10 Hz). A non-linearity of <1.3% full-scale output (FSO) is measured. The bias current used in measuring, the response to DC magnetic field is 10 mA, 400 Hz. Non-linearity in this case is better than 2% FSO. Finally, in measuring response to the ac magnetic field, a bias current of 10 mA, 1000 Hz is used and an m-linearity of <0.7 % is demonstrated.

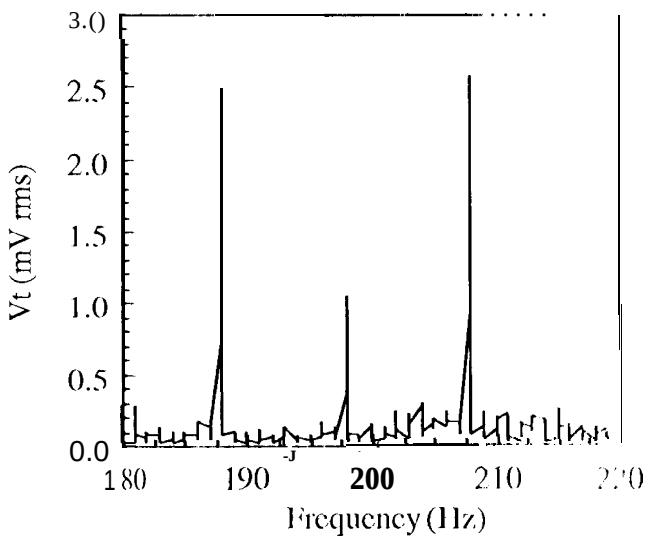

Figure 3. Output spectral response of a tunneling μ-magnetometer to DC (peak at f = 196 Hz) and ac (peaks at f = 196 ± 10 Hz) magnetic fields.

In addition to linearity measurements, responsivity measurements were taken and compared to theoretical values. Since the tunneling μ-magnetometer is controlled by a force-rebalance feedback loop the responsivity can be calculated by equating the responses of the Lorentz force and the electrostatic forces to the magnetic field. The responsivity of the tunneling μ-magnetometer can then be expressed as:

$$\frac{\partial Vt}{\partial B} = \frac{nIld^2}{\varepsilon_0 A V_{def}}, \qquad (3)$$

where d is the spacing between the electrostatic actuator electrodes, ε_0 is the permittivity of free space, A is the area of the electrostatic actuator electrode and V_{def} is the static voltage applied at the onset of tunneling. A theoretical responsivity value of 3.44 V/T is in excellent agreement with the experimental value of 3.15 V/T. Note that the responsivity is calculated exclusively from the device structure and not from any fitted parameters. Also note that the responsivity can be increased dramatically by adjusting the device design.

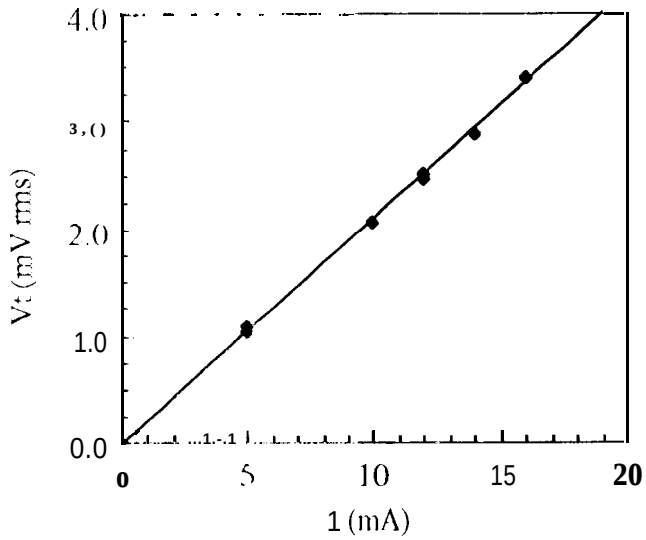

Figure 4. Output response of tunneling μ-magnetometer to increasing bias current. Incident magnetic field, B = 900 μT, 10 Hz. Non-linearity < 1.3 % FSO.

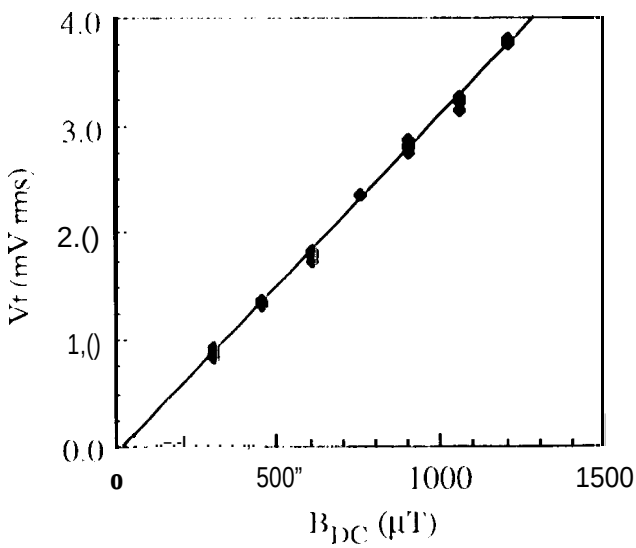

Figure 5. Output response of tunneling μ-magnetometer to increasing DC magnetic field. Bias current, I = 10 mA, 400 Hz. Non-linearity < 2 % FSO.

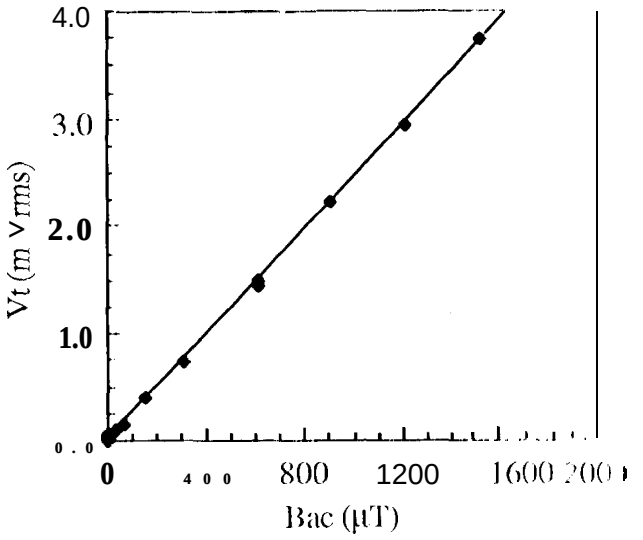

Figure 6. Output response of tunneling μ-magnetometer to increasing ac magnetic field. Bias current, I = 10 mA, 10001 Hz. Non-linearity < 0.7 % FSO

OPTIMIZED DESIGN

Given the excellent agreement between the device performance model and the measured operation of the prototype, producing an optimized tunneling μ-magnetometer is can be easily accomplished from Equation 3, NEB can be improved by 700X by adjusting the. device structure and operating point. For example, the Lorentz force can be greatly increased for a given magnetic field by increasing the number of loops in the wire coil (n) from 1 to 30 and increasing, the dimension of the flexible silicon nitride membrane (L) from 2.5 X 2.5 mm^2 to 5 X 5 mm^2: 60 X overall improvement in NEB. By pushing the operating point out from 200Hz to 10001 Hz, the voltage noise. is reduced from 35 μV/√Hz to 10 μV/√Hz 3.5 X improvement in NEB. Finally, by increasing the current in the wire coil from 10 mA to 33 mA another 3.3 X improvement in NEB is produced. The cumulative effect is to reduce the. NEB from 2.8 μV/√Hz to 4 nT/√Hz by systematically adjusting the design and operating point of the tunneling magnetometer while maintaining small size (1 cm^3) and low power (<100 mW). This design is currently being fabricated.

CONCLUSIONS

A prototype μ-magnetometer has been designed, fabricated and characterized for use in small-spacecraft and commercial applications. The tunneling μ-magnetometer is fabricated exclusively from silicon using bulk micromachining techniques to produce a microelectromechanical sensor which monitors minute changes in a Lorentz force. The Lorentz force is induced by the interaction between a magnetic field and a current loop supported on a flexible membrane on the device. An electron tunneling transducer is utilized to monitor the displacement of the membrane in response to the Lorentz force using a force rebalance network. Linearity, responsivity and noise equivalent magnetic field (NEB) measurements are in excellent agreement with a device performance model. Using the device model, an optimized device design is in progress to improve the NEB of the. ~~-magnetometer by adjusting simple device parameters. For example, by adjusting the device design parameters to n = 30 loops, I(1kHz) = 33mA, and L = 5111111 X 5 mm, an NEB of 4nT/√Hz is achievable. This design also maintains the low power, and small size requirements necessary for μ-spacecraft and commercial applications.

ACKNOWLEDGMENTS

The authors would like to thank J. Randolph, R. Goldstein, for helpful technical (discussions and for their leadership in the development of the free flying magnetometer. The authors also wish to thank G. Chen, H. Javadi, M. Hoenk, S. Manion, H. Rockstad, J. Schroeder, T. Tang, T. VanZandt, E. Vote for technical discussions; R. Muller, and P. Maker for e-beam support; and L. Kirk, S. Lewis and A. Lumb for testing support. The research described in this paper was performed by the Center for Space Microelectronics Technology, Jet Propulsion Laboratory, California Institute of Technology, and was jointly sponsored by Eaton Corporation and the National Aeronautics and Space Administration, Office of Space Access and Technology.

REFERENCES

[1] 1.. Muller, M. 11. Hecht, L. M. Miller, J C. Lyke, "Packaging and Qualification ofN41 3MS 1 Based *Space* Systems, *IEEE Workshop on Micro Electro Mechanical Systems, 1 Feb. 11-15,* 1996.

[2] J. Clark, "Advances in SQUID magnetometers", *IEEE Trans. Electron Devices*, vol. ED- 2'/, No 10 1, pp. 1896-1908, 1980.

[3] J. Wikswo, Jr., "SQUID Magnetometers for Biomagnetism and Nondestructive Testing: Important Questions and initial Answers", *IEEE Trans Appl. Superconductivity*, Vol. **5, No. 2,** pp. 74-120. 1 995.

[4] J. E. Lenz, "A Review of Magnetic Sensors' 1'1"0[". *IEEE*, vol. 70, No. 6, pp. 973-989, 1990.

[5] T. W. **Kenny,** W. J. Kaiser, 11. K. Rockstad, J. K. Reynolds, J. A. Podosek, and E. C. **Vote,** "Wide -bandwidth electromechanical actuators for tunneling displacement transducers", *J. Microelectromech. Syst.*, Vol. 3, No. 3, pp. 97-104, 1994.

[6] 11. K. Rockstad, '1'. W. Kenny, J. K. Reynolds, and W. J. Kaiser, "A miniature high-sensitivity broad-band accelerometer based on electron tunneling transducers", *Sensors and Actuators A,* Vol. 43, pp. 107- 114, 1994.

[7] **'1'.** W. Kenny, J. K. Reynolds, J. A. Podosek, E. C. Vote, L. M. Miller, 11. K. Rockstad, and W. J. Kaiser, "Micromachined Infrared Sensors using Tunneling 1 Displacement Transducer", Rev. *Sci. Instruments*, Jan., 1 996.

[8] G. Binnig and 11. Rohrer, "Scanning Tunneling Microscopy", *IBM J. Res. Dev.*, Vol. 30, pp. 355-369, 1982.